JOURNAL OF VIROLOGY, Mar. 1991, p. 1466–1478
0022-538X/91/031466-13$02.00/0

Vol. 65, No. 3

Functional Domains of Epstein-Barr Virus Nuclear Antigen EBNA-1

RICHARD F. AMBINDER,[1] MARYANN MULLEN,[1] YUNG-NIEN CHANG,[1]
GARY S. HAYWARD,[1] AND S. DIANE HAYWARD[1,2]*

The Virology Laboratories, Department of Pharmacology and Molecular Sciences[1] and Department of Neurology,[2] Johns Hopkins School of Medicine, 725 North Wolfe Street, Baltimore, Maryland 21205

Received 23 August 1990/Accepted 15 November 1990

The Epstein-Barr virus (EBV)-encoded latency product EBNA-1 is functionally pleiotropic, being required for replication of the episomal form of the EBV genome and having a role in the regulation of latency transcription. EBNA-1 is a direct DNA-binding protein, and both replication and transactivation are dependent on the interaction of EBNA-1 with its cognate DNA recognition sequences. To better understand EBNA-1 function, we have further characterized the DNA-binding domain of EBNA-1 and have examined the contributions of other domains of the protein to EBNA-1 transactivation activity. A *Bal*31 deletional analysis of the carboxy-terminal region of EBNA-1 identified a core DNA-binding domain located between amino acids 493 and 584. Column chromatographic, sedimentation, and cross-linking studies indicated that EBNA-1 exists in solution as a dimer. Mobility retardation assays using in vitro-translated variants of EBNA-1 showed that the active DNA-binding form of EBNA-1 is also a dimer. In short-term cotransfections, a pFRTK-CAT target containing EBNA-1-binding sites from the EBV origin of plasmid replication, ori-P, was transactivated by a carboxy-terminal EBNA-1 construction (amino acids 450 to 641) that also carried a c-*myc* nuclear localization signal. These reconstruction experiments demonstrated that a transactivation domain exists within the carboxy-terminal region of EBNA-1, that transactivation is more efficient when a nuclear localization signal is present, and that the natural karyophilic signal lies outside of the carboxy-terminal 191 amino acids. To identify the EBNA-1 nuclear localization signal, small oligonucleotides representing EBNA-1 sequences that encode clusters of basic peptides were transferred into two different vectors expressing cytoplasmic proteins (pyruvate kinase and herpes simplex virus ΔIE175 protein) and the cellular locations of the fusion constructions were determined by immunofluorescence staining of transfected cells. In this way we identified a functional nuclear localization signal, Leu-Lys-Arg-Pro-Arg-Ser-Pro-Ser-Ser, encompassing amino acids 379 to 386 of the EBNA-1 protein.

All herpesviruses share the ability to establish a latent infection in their hosts. In the case of Epstein-Barr virus (EBV), latency is established in B-cells and viral gene expression is limited to the six members of the EBNA family of nuclear proteins, two membrane proteins, and two small polymerase III transcripts (reviewed in reference 17). In the latently infected B cell, EBV genomes exist predominantly as extrachromosomal episomes whose replication is synchronized with cell division (21, 27). Integrated genomes may also be present (20, 24). A plasmid DNA molecule carrying the latency origin of replication, ori-P, will replicate episomally in DNA transfected cells provided that the viral product EBNA-1 is also provided in *trans* (22, 43, 45). This result indicates that EBNA-1 is the only viral protein necessary for the latent form of EBV replication, all other functions being provided by the host. The cell type affects replication ability. Episomal replication is observed in DNA-transfected human and simian cells but not in rodent cells (45). This may indicate a requirement for EBNA-1 to interact with the cellular replication machinery.

Ori-P consists of two components: the family of repeats, which comprises 20 tandem copies of a 30-bp element, and the dyad symmetry, which contains 4 copies of the repeat. These copies are separated by 980 bp of spacer DNA (33, 43). The dyad symmetry is the site of initiation of episomal DNA replication (11, 42), while the family of repeats acts as an EBNA-1-dependent enhancer when linked to plasmid constructions such as TK-CAT or A10-CAT (33, 34). Biological activity is retained when the copy number of the family of repeats is reduced experimentally to seven, but not when it is reduced below this number (6, 42). In addition to the contribution of the family of repeats to origin function, Sugden and Warren (40) showed that the EBV *Bam*HI-C latency promoter is transactivated by EBNA-1 through the ori-P tandem repeats acting as an enhancer region. Thus EBNA-1 also has a role in regulation of expression of the EBNA family of latency genes. As a consequence of its replication and transcriptional activation functions, EBNA-1 plays a central role in the maintenance of viral latency.

EBNA-1 interaction with ori-P is mediated via direct binding to DNA elements in the family of repeats and dyad symmetry loci (15, 32). A third EBNA-1-binding locus of unknown function occurs in a separate region of the genome in *Bam*HI-Q (3, 32). The differential affinity of EBNA-1 for these three loci may contribute to its ability to modulate both latency replication and transcriptional activity. The family of repeats has a higher affinity for EBNA-1 than does the dyad symmetry, and the Q locus has the lowest affinity (15). The differences in affinity are principally a consequence of primary DNA sequence variations that occur in individual binding sites within the dyad symmetry and Q loci (3). EBNA-1 binds tightly to its specific DNA target, and the K_d for a consensus binding site is 1×10^{-11} to 2×10^{-11} M (3).

EBNA-1 is transcribed as a highly spliced message from the latency promoters in *Bam*HI-C and *Bam*HI-W that lie 80 to 90 kb upstream from the EBNA-1 open reading frame (bp 107,950 to 109,872 [9, 36, 39, 41]). A limited amount of information exists on the domain structure of EBNA-1. The 641-amino-acid (aa) EBNA-1 polypeptide contains a central

* Corresponding author.

domain, aa 90 to 328, that is composed entirely of a repetitive array of glycine and alanine residues. EBNA-1 polypeptides in which the majority of this domain is deleted function as well as, if not better than, intact EBNA-1 in transactivation, transient replication, and plasmid maintenance assays (30, 44, 45). We had previously shown that the DNA-binding domain of EBNA-1 lies within the carboxy-terminal 191 aa (3, 32). A bacterially expressed fusion polypeptide that included EBNA-1 aa 450 to 641 bound specifically to EBNA-1 target sequences within ori-P and gave a footprint essentially identical to that obtained with the intact protein (15). Both EBNA-1-dependent DNA replication and transactivation functions are ablated by deletions within this carboxy-terminal region (22, 30, 44).

Mapping of other functional domains of EBNA-1 has previously been undertaken through the introduction of deletions into the EBNA-1 coding sequence. However, analysis of the results obtained by this approach was somewhat complicated by the multifactorial nature of replication and transactivation. These activities are likely to require that the protein localizes correctly to the nucleus, is capable of binding DNA, and retains an activator domain. We have sought to further characterize the functional domains of EBNA-1 by using a combination of deletional analysis and protein dissection. Since DNA binding is an absolute requirement, we first sought to better define the limits of the DNA-binding domain and to investigate the nature of the EBNA-1–DNA interaction. We then examined the properties of transactivation and nuclear localization. These experiments defined a minimal DNA-binding domain, determined that EBNA-1 binds DNA as a dimer, and suggested that EBNA-1 may contain two distinct activation domains. The negative tail of EBNA-1, comprising aa 600 to 641, which is not essential for transactivation by an otherwise intact protein, contributed to transactivation by the truncated aa 450 to 641 EBNA-1 construction. The ability to localize appropriately to the nucleus also contributed to transactivation ability, and we identified an EBNA-1 nuclear localization signal comprising the amino acids Leu-Lys-Arg-Pro-Arg-Ser-Pro-Ser-Ser.

MATERIALS AND METHODS

Plasmid constructions. Three series of plasmids capable of expressing EBNA-1 polypeptides in eukaryotic cells were generated. The parental plasmid in the first series was pRA17, in which the complete EBNA-1 coding sequence was placed behind the immediate-early promoter of simian cytomegalovirus. A *Bam*HI-*Hin*dIII fragment containing EBV (B95-8) DNA sequences 107,565 to 110,496 was inserted behind the simian cytomegalovirus promoter in pTJ278 (14). A *Sal*I-*Eco*RI fragment containing the promoter and EBNA-1 sequences was then ligated into *Sal*I-*Eco*RI-cleaved BlueScribe M13 (+) (Stratagene, La Jolla, Calif.). pRA31 was generated by partial digestion of pRA17 with *Sma*I and introduction of an *Xba*I linker. This resulted in a frameshift mutation with no EBNA-1 sequences being expressed beyond codon 429. Plasmids pRA35 and pRA37 were the products of partial digestion of pRA17 with *Hpa*II followed by ligation in the presence of *Kpn*I linkers. These in-frame deletions removed codons 390 to 547 and 329 to 345, respectively. pRA20 was created by cleavage of pRA17 with *Sst*II, formation of blunt ends, and introduction of an *Xba*I triple terminator oligonucleotide (5′-CTAGTCTA GACTAG-3′).

The second series of plasmids was based on pRLPK12, which contains the coding sequences for chicken pyruvate kinase under the control of the simian virus 40 early promoter (7). pRA315 contains the nuclear localization signal from the c-*myc* oncogene (Pro-Ala-Ala-Lys-Arg-Val-Lys-Leu-Asp) cloned between the *Xho*I and *Eco*RI sites at codon 12 of pRLPK12 (7). pRA326 has the *Bam*HI site in the vector sequences of pRLPK12 removed by *Bam*HI cleavage. This removal is followed by filling in with Klenow polymerase and religation, and the *Xho*I and *Eco*RI sites used for insertion of the nuclear localization signal are converted to a single *Bam*HI site. In pRA321, the *Kpn*I site at codon 443 of pyruvate kinase in pRLPK12 was converted into a *Bam*HI site by linker insertion, and a 2.2-kb fragment containing EBNA-1 codons 450 to 641 plus downstream sequences was removed from pNAK28 (26) into the *Bam*HI site. The translational termination and polyadenylation signals in pRA321 are provided by the natural EBNA-1 sequences. pRA336 was created by ligating the *Eco*RI-*Bam*HI fragment of pRA315 that contains the beginning of the pyruvate kinase cDNA and the c-*myc* nuclear localization signal to the *Eco*RI-*Bgl*II fragment of pRA321 that contains the remainder of the pyruvate kinase cDNA fused to the carboxy terminus of EBNA-1. In pRA357 the EBNA-1 insert of pRA336 was replaced with an equivalent 2.2-kb *Bam*HI fragment that contained an *Xba*I triple terminator inserted at the *Sst*II site and expressed EBNA-1 aa 450 to 619. Oligonucleotides encoding potential nuclear localization signals were inserted at codon 12 of pyruvate kinase between the *Xho*I and *Eco*RI sites of pRLPK12 or at the *Bam*HI site of pRA326. The oligonucleotides 5′-TCGAGGGCAGGCGC AAAAAAGGAG-3′ and 5′-AATTCTCCTTTTTTGCGCCT GCCC-3′ were annealed and inserted to form pRA298. The target plasmid pFRTK-CAT used in transactivation assays was a gift from B. Sugden (33).

The parental plasmid in the third series was pGH115, which expresses a cytoplasmic variant of the immediate-early IE175 protein of herpes simplex virus (HSV). In the protein expressed by pGH115, aa 353 to 833 are deleted from the original 1,298-aa IE175 protein. This was accomplished by taking the IE175-expressing plasmid pGH114, creating an internal deletion between the *Stu*I sites, and inserting a 12-mer *Bgl*II linker. The following oligonucleotide pairs were annealed, and the double-stranded products were ligated into *Bgl*II-cleaved pGH115 in both forward (a) and backward (b) orientations: pMAH9a and pMAH9b, 5′-GATCCGGAGACCCCAAAAACGTCCACA-3 and 5′-GAT CTGTGGACGTTTTTGGGGTCTCCG-3′; pMAH10a and pMAH10b, 5′-GATCCTTAAGAGGCCCAGGAGTCCCAG TAGTCA-3′ and 5′-GATCTGACTACTGGGACTCCTGG GCCTCTTAAG-3; pMM15a and pMM15b, 5′-GATCCT TTCTCCACCGCGCAGGCCCCCTCCAGGTAGAAGGCC ACA-3′ and 5′-GATCTGTGGCCTTCTACCTGGAGGGGG CCTGCGCGGTGGAGAAAG-3′.

Plasmid pRA362 formed the template for in vitro transcription of EBNA-1. The polymerase chain reaction was used to generate a DNA fragment that encoded aa 408 to 641 of EBNA-1. This fragment was cloned between the *Bam*HI and *Eco*RI sites of the RNA expression vector pBD7 (8) to form pRA362.

The 5′ *Bal*31 deletion series was created in a bacterial EBNA-1 expression vector by cleavage of pRA17 with *Sma*I followed by digestion with *Bal*31 nuclease for 2, 5, 10, 15, and 20 min. After phenol-chloroform extraction and ethanol precipitation, the DNA was digested with *Sal*I, the ends were blunted, and the plasmid was religated. This protocol resulted in a series of deletions around the *Sma*I site at aa

450 of EBNA-1 being fused to the *lacZ* promoter and polylinker region of the BlueScribe plasmid. The 3′ *Bal*31 deletions were generated in a similar manner, using a starting plasmid that had an *Xba*I linker inserted at the *Sst*II site at codon 619 of EBNA-1. A partial *Sma*I digestion resulted in two vector plasmids, one initiating the EBNA-1 polypeptide at aa 430 and the other initiating at aa 450. The vectors were cleaved at the introduced *Xba*I site, and after digestion with *Bal*31 nuclease, *Eco*RI linkers were added and the plasmids were religated. The deletion endpoints of the resulting plasmids were determined by sequencing, and selected members of the deletion series were moved as *Pst*I-*Eco*RI fragments into a λNp bacterial expression vector (pHE6) to obtain better expression of the EBNA-1 polypeptides. The original pHE6 plasmid (26) was modified for this purpose such that the *Bam*HI polylinker site was converted to a *Pst*I site and the original *Pst*I polylinker site was converted to an *Eco*RI site.

DNA-binding assays. Preparation of bacterially expressed EBNA-1 fusion proteins, DNA-protein-binding reactions, and mobility retardation assays were performed as previously described (3). The 30-mer oligonucleotide substrate for the DNA-binding assay was oligonucleotide 20, containing a single consensus palindromic EBNA-1-binding site (3). EBNA-1 was also prepared by in vitro transcription-translation from pRA362, which was linearized either downstream of the coding region with *Eco*RI or internally with *Sst*II to generate a truncated peptide. The linearized plasmid was incubated with T7 RNA polymerase to generate capped mRNA in a commercial protocol (Stratagene). In vitro translation was carried out by using a nuclease-treated rabbit reticulocyte lysate (Promega, Madison, Wis.) in the presence of RNasin RNase inhibitor and [^{35}S]methionine according to the manufacturer's protocol. RNA products were analyzed on denaturing 1% agarose gels (23), and protein products were analyzed on 10% denaturing polyacrylamide gels. After incubation of the probe with the in vitro-translated EBNA-1 and electrophoretic separation of the bound complexes, the gel was exposed to two layers of X-ray film. The intervening layer was necessary to screen out the autoradiography contributed by the ^{35}S-labeled EBNA-1 protein.

High-pressure liquid chromatography (HPLC), glycerol gradients, and cross-linking. EBNA-1 fusion protein (100 μl) that had been partially purified by DEAE-cellulose and heparin agarose column chromatography (15) was applied to a Beckman Spherogel TSK 3000SW column (7.5 by 300 mm) equilibrated in column buffer (50 mM HEPES [*N*-2-hydroxyethylpiperazine-*N*′-2-ethanesulfonic acid; pH 7.5], 25 mM $MgCl_2$, 2 mM dithiothreitol, 0.2 mM EDTA, 0.2 mM phenylmethylsulfonyl fluoride, 20 mM sodium metabisulfate, 100 mM KCl) adjusted to 400 mM KCl. EBNA-1 was eluted at a rate of 1 ml/min, and the eluant was monitored by spectrophotometric absorption at 280 nm. Fractions (0.25 ml) were collected, and 10-μl aliquots were tested for specific DNA-binding activity by using the mobility retardation assay. The column was calibrated with a mixture of standard marker proteins: bovine thyroglobulin (670 kDa), bovine gamma globulin (158 kDa), chicken ovalbumin (44 kDa), horse myoglobin (17 kDa), and vitamin B_{12} (1.3 kDa) (Bio-Rad, Richmond, Calif.). Elution of the protein standards was also monitored by A_{280}. The EBNA-1 fusion protein (120 μl) was also analyzed by sedimentation through a 4-ml 10 to 30% glycerol gradient containing column buffer. Parallel glycerol gradients were loaded with bovine serum albumin and alcohol dehydrogenase marker proteins. The gradients were centrifuged in a Sorvall TST 60.4 swinging-bucket rotor for 24 h at 4°C and 40,000 rpm. Fractions (200 μl) were collected from the top of the tubes, and an aliquot (10 μl) of each fraction of the EBNA-1 gradient was assayed for specific DNA-binding activity by using the mobility retardation assay. The positions of the protein standards were determined by the Bradford assay (Bio-Rad). Glutaraldehyde cross-linking of in vitro-translated EBNA-1 and analysis of the products of the reaction on sodium dodecyl sulfate (SDS)-polyacrylamide gels were performed as previously described (4). Immunoprecipitation of EBNA-1 utilized a rabbit serum raised against the bacterially expressed EBNA-1 fusion protein (26).

DNA transfection, CAT assays, and immunofluorescence assays. Vero and cos-7 cells were grown in Dulbecco modified Eagle minimal essential medium (DMEM) supplemented with 10% fetal calf serum. For chloramphenicol transferase (CAT) assays, Vero cells were plated in six-well cluster dishes at 2×10^5 cells per well the day before transfection and were transfected by the calcium phosphate-BES [*N*,*N*-bis(2-hydroxyethyl)-2-aminoethanesulfonic acid]-buffered saline procedure (5). Cells were harvested 40 h after transfection, and CAT assays were performed as previously described (28).

For immunofluorescence assays, cos-7 or Vero cells were seeded onto slides (LabTek Products) the day before transfection. Cells were transfected with 1 to 2 μg of plasmid DNA by either the BES-buffered saline modification of the calcium phosphate precipitation method (Vero cells) or, in the case of cos-7 cells, by the original calcium phosphate precipitation procedure (28). Forty-eight hours after transfection, slides were rinsed in Tris-saline (25 mM Tris [pH 7.5], 138 mM NaCl, 2 mM MgCl, 1 mM $CaCl_2$) and fixed in cold absolute methanol for 10 min (EBNA-1 or IE175) or 3.5% paraformaldehyde (pyruvate kinase). After rehydration in Tris-saline, the slides were incubated with the first antibody for 45 min at 37°C in a humidified chamber, washed in Tris-saline, and incubated with the appropriate fluorescein-conjugated second antibody for 30 min at 37°C. Immunological reagents were 58S, a mouse monoclonal antibody to the HSV type 1 (HSV-1) IE175 protein (37), used at a 1:50 dilution; rabbit serum raised against chicken muscle pyruvate kinase that was purchased commercially (Sigma Chemical Co.), used at a 1:50 dilution; and human anti-EBNA-1 serum from patients with nasopharyngeal carcinoma, used at a 1:100 dilution. (In the case of this last serum, the protocol included an intermediate step in which the slides were incubated for 30 min at 37°C with human complement diluted 1:20.) The fluorescein-conjugated antibodies were goat anti-human C3, goat anti-rabbit immunoglobulin G, and goat anti mouse immunoglobulin G, all obtained from Organon Teknika-Cappel, Malvern, Pa. Slides were viewed and photographed with a Leitz fluorescence microscope.

RESULTS

Defining the boundaries of the DNA-binding domain. Previous studies had shown that a bacterially expressed fusion protein containing the carboxy-terminal 191 aa of EBNA-1 bound to DNA targets containing EBNA-1 recognition sites in a manner equivalent to that of the intact EBNA-1 protein (3, 15, 25, 32). These data indicated that the DNA-binding domain of EBNA-1 lay within the carboxy-terminal one-third of the protein. As a step towards characterization of the interaction between EBNA-1 and its DNA target, we sought to determine the minimal domain of EBNA-1 that was

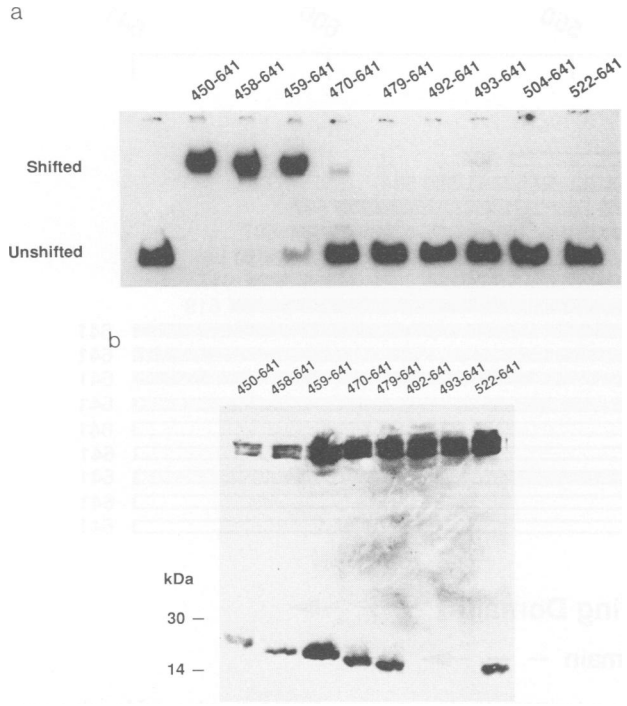

FIG. 1. Definition of the 5′ boundary of the DNA-binding domain. (a) Mobility retardation assay using a 30-mer-oligonucleotide-binding site as probe and bacterially expressed fusion polypeptides containing the indicated amino acid residues of EBNA-1. The first lane shows the position of probe DNA in the absence of added EBNA-1 extract. (b) Immunoblot analysis of protein expression from the 5′ deletion constructions. Bacterial extracts were electrophoresed through a denaturing 10% SDS-polyacrylamide gel, transferred to nitrocellulose, and incubated with rabbit anti-EBNA-1 antiserum (26). The reactive bands were visualized by incubation with protein A-gold followed by silver enhancement (Bio-Rad).

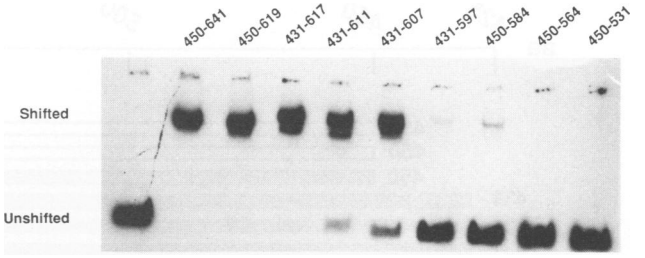

FIG. 2. Definition of the 3′ boundary of the DNA-binding domain. Mobility retardation assay performed with the same probe as used for Fig. 1 and bacterially expressed EBNA-1 polypeptides that were deleted for carboxy-terminal amino acids. The first lane shows the position of the probe DNA in the absence of added EBNA-1 extract.

capable of specific DNA binding. A series of 5′ and 3′ *Bal*31 deletions were introduced into a vector that expressed the carboxy-terminal 191 aa of EBNA-1 (aa 450 to 641) as a fusion product with 26 aa of *lacZ*. Following *Bal*31 nuclease treatment, we identified 22 5′ deletions and 13 3′ deletions of the DNA-binding domain, and the endpoints of these deletions were determined by DNA sequencing (2). However, the *lacZ* fusion vector did not give satisfactory yields of EBNA-1, and to remedy this situation, selected members of the deletion series were moved into the λN bacterial expression vector that we had previously exploited for studies of EBNA-1 (3, 26, 32).

The ability of eight of the transferred 5′ deletions to bind to DNA was compared with that of the original aa 450 to 641 polypeptide (450-641 polypeptide) in mobility retardation assays by using a synthetic 30-mer oligonucleotide binding site as the substrate (Fig. 1a). DNA binding comparable to that of the 450-641 polypeptide was retained by the 458-641 and 459-641 constructions, and weaker DNA binding was exhibited by the 470-641 polypeptide. DNA binding was barely detectable (approximately one-fifth of the binding of the 470-641 polypeptide) when the 5′ terminus was located at amino acid 479 or 492, and weak binding was restored in the 493-641 polypeptide. DNA binding was completely lost when the deletion extended to or beyond aa 504. Immunoblot analysis (Fig. 1b) of the bacterial extracts used in the mobility shift assay indicated that several factors contributed to loss of DNA binding. Disruption of protein conformation may be a factor in the cases of the 470-641 and 479-641 polypeptides. Both were stable on the basis of immunoblot analyses but gave only weak (470-641 polypeptide) or barely detectable (479-641 polypeptide) binding. Deletion into the region around aa 492 clearly destabilizes the polypeptide product, as indicated by the fact that 492-641 and 493-641 polypeptides cannot be detected on an immunoblot. However, the exquisite sensitivity of the mobility shift assay is such that weak EBNA-1 binding can still be measured in the case of the 493-641 polypeptide. Stability is restored in the 522-641 construction, but this polypeptide has no DNA-binding activity, and no restoration of binding occurred with more-extensive 5′ deletions.

Eight 3′ deletions were also transferred into the λN vector, and the polypeptide products were similarly tested for their abilities to bind to the 30-mer oligonucleotide target. The 3′ deletions were derived from two separate series, one initiating at aa 450 and the second initiating at aa 431. As demonstrated in a mobility shift assay (Fig. 2), strong specific binding was retained when the carboxy boundary was moved from the natural terminus at aa 641 back to aa 607. Weak binding was exhibited by the variants terminating at aa 597 and 584, and binding was undetectable when the EBNA-1 polypeptide was terminated at or internal to aa 564. The aa 607 position apparently demarcates a protein stability boundary, since the polypeptides terminating at aa 641, 619, 617, 611, and 607 were detectable by immunoblot analyses, whereas those terminating internally to aa 607, i.e., at aa 597, 584, 564, and 531, were not (data not shown). In summary, the 5′ and 3′ boundaries for retention of wild-type levels of DNA-binding activity were defined by the 459-641 and 431-607 polypeptides. Loss of DNA binding upon further deletion appears to result from a combination of three factors, i.e., loss of polypeptide stability, perturbation of protein conformation, and intrusion into the motifs that constitute the DNA-binding domains themselves. The abilities of the 493-641 and 450-584 polypeptides to retain detectable, if reduced, binding activity suggest that a core binding domain is located within aa 493 to 584 of EBNA-1 (Fig. 3).

EBNA-1 dimerizes in solution and binds to DNA as a dimer. The majority of proteins that interact with specific DNA sequences bind to their targets as dimers or higher-order multimers. To examine the subunit structure of EBNA-1, we undertook several approaches, namely, sizing analyses using gel filtration, velocity gradient sedimentation, and cross-linking, along with binding analyses using coexpressed large and small variants of EBNA-1. The apparent molecular

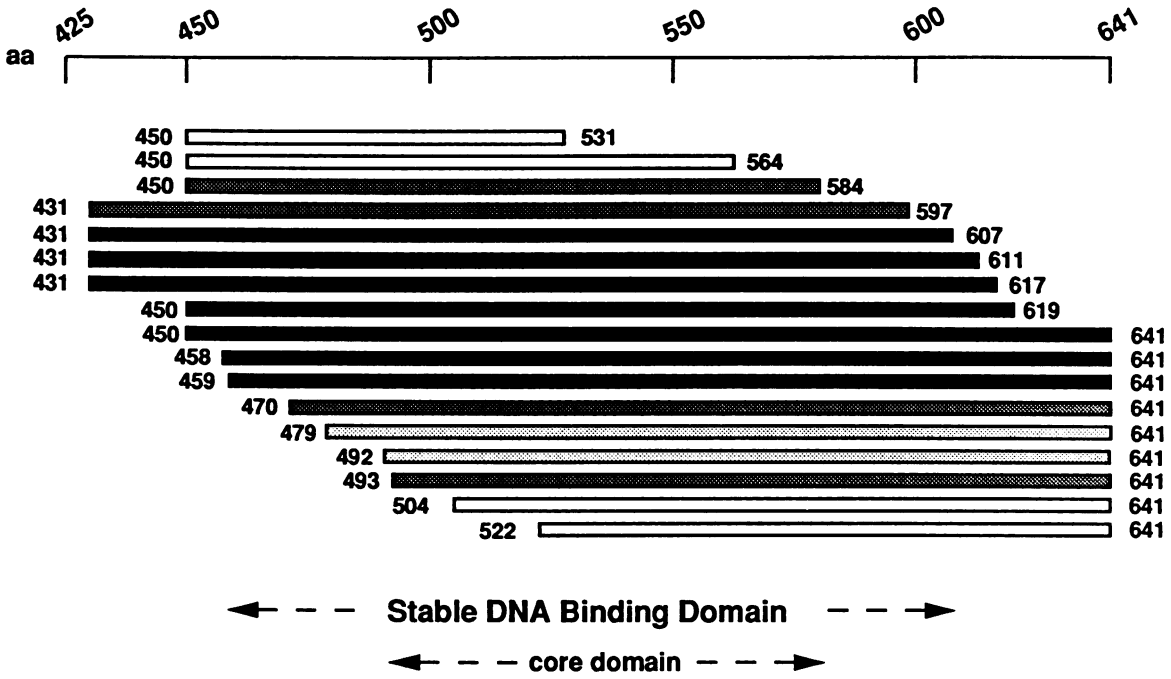

FIG. 3. Summary of the *Bal*31 deletional analyses performed to locate the DNA-binding domain. EBNA-1 polypeptides that gave wild-type levels of binding are indicated by solid bars, those that bound weakly are indicated by heavily stippled bars (10% of wild-type binding) or lightly stippled bars (2% of wild-type binding), and nonbinders are shown as open bars. These constructions locate a stable DNA-binding domain with wild-type activity between aa 459 and 607 and suggest that a core-binding domain exists within the aa 493 to 584 segment of EBNA-1.

weight in solution of the bacterially expressed 28,000-molecular weight EBNA-1 fusion protein (28K protein) containing EBNA-1 aa 450 to 641 was first determined by size exclusion HPLC using a Spherogel TSK 3000SW column and 28K EBNA-1 which had been purified by chromatography on DEAE-cellulose and heparin agarose columns. Eluant from the HPLC sizing column was monitored by spectrophotometric absorption at 280 nm, and fractions (0.25 ml) were collected. A portion (10 μl) of each fraction was assayed for DNA-binding activity by using the mobility retardation assay. A_{280} and DNA-binding activity both peaked in the 7.0- to 7.25-ml fractions (Fig. 4) corresponding to an apparent molecular mass in the 50- to 70-kDa range. The 28K EBNA-1 was also sedimented through a 10 to 30% glycerol gradient, and its sedimentation profile was compared with those of bovine serum albumin and alcohol dehydrogenase marker proteins. The gradients were fractionated into 200-μl aliquots, and a sample (10 μl) of each fraction of the EBNA-1 gradient was again assayed for DNA-binding activity. In this case, binding activity peaked in fractions 9 and 10, which correspond to a molecular mass of 53 to 70 kDa (Fig. 5). The molecular mass of 28K EBNA-1 predicted from its amino acid composition and from its migration in SDS-polyacrylamide gels is 28 kDa. Therefore, the behavior of the protein on the HPLC sizing column and on the glycerol gradient is consistent with the 28K EBNA-1 protein existing in solution as a stable dimer of 28-kDa subunits.

To obtain further confirmation of this stoichiometry, a cross-linking experiment was performed with an EBNA-1 polypeptide (aa 406 to 641) synthesized by in vitro transcription-translation. The ^{35}S-labeled EBNA-1 was immunoprecipitated with anti-EBNA-1 rabbit antiserum either before or after being cross-linked with glutaraldehyde and subjected to SDS-polyacrylamide gel electrophoresis (Fig. 6a). In the absence of cross-linking, the EBNA-1 peptide migrated with a molecular mass of approximately 30 kDa. Glutaraldehyde treatment resulted in the appearance of an additional 70-kDa polypeptide species. This experiment therefore provided additional evidence that EBNA-1 exists in solution as a dimer.

To determine whether the EBNA-1 dimer was the active DNA-binding form, we utilized the heterodimerization approach originated by Hope and Struhl (13). Two EBNA-1 polypeptides of different sizes were generated by using the in vitro transcription-translation system. The larger polypeptide contained aa 406 to 641 of EBNA-1, while the smaller polypeptide (Δ22) lacked the carboxy-terminal 22 amino acids. Both EBNA-1 variants bound to a 30-mer oligonucleotide probe, but as expected, the complex formed between the smaller Δ22 EBNA-1 and the probe migrated further into the gel in a mobility retardation assay than did the complex containing the larger EBNA-1 variant (Fig. 6b, lanes 1 and 2). When these two forms of EBNA-1 were cotranslated, a complex with intermediate mobility was observed in addition to the two original DNA-protein complexes. The presence of three shifted complexes is indicative of the formation of dimers consisting of large-large, large-small, and small-small EBNA-1 proteins. Thus, the active DNA-binding form of EBNA-1 is also a dimer.

Carboxy-terminal 191 aa do not contain a nuclear localization signal. Deletional analyses have previously demonstrated that a carboxy-terminal region of EBNA-1 that included the DNA-binding domain was necessary for EBNA-1 transactivation function (30, 44). We were interested in determining whether the carboxy-terminal 191 aa were sufficient for transactivation, i.e., whether this region

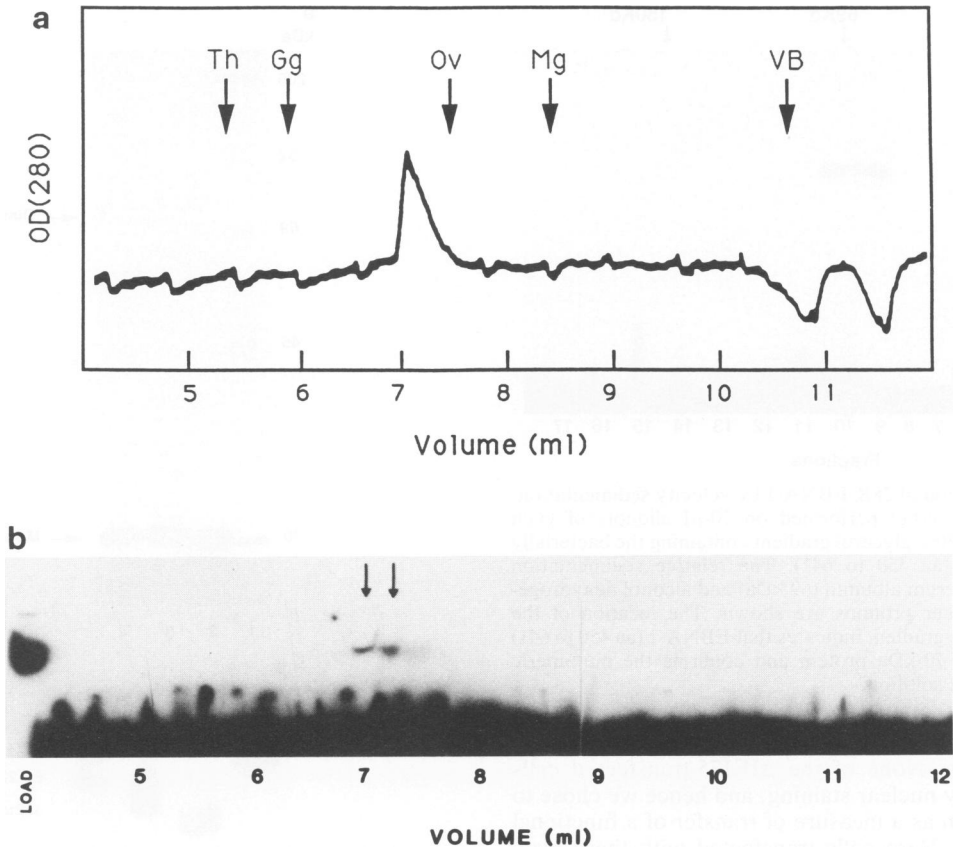

FIG. 4. Examination of 28K EBNA-1 by size exclusion chromatography. (a) A partially purified preparation of bacterially expressed EBNA-1 (aa 450 to 641) was passed over a Spherogel TSK 3000SW size exclusion column. A single peak (optical density at 280 nm) [OD(280)] was present in the 7.0- and 7.25-ml fractions. The relative elution positions of a mixture of standard marker proteins are also indicated. Th, Thyroglobulin (670 kDa); Ga, gamma globulin (158 kDa); Ov, ovalbumin (44 kDa); Mg, myoglobin (17 kDa); VB, vitamin B_{12} (1.3 kDa). (b) Mobility retardation assay performed using a 30-mer EBNA-1 oligonucleotide probe and 10-μl samples from each column fraction. The DNA-binding activity coincided with the optical density (280 nm) peak and indicated that 28K EBNA-1 exists as a 50- to 70-kDa multimeric form in solution.

contained an activator domain in addition to the DNA-binding domain. Before we addressed this question experimentally, there was an additional factor to be considered. EBNA-1 is a nuclear protein, and a cotransfection assay for transactivation function of the 450-641 polypeptide would be valid only if this polypeptide retained the ability to localize normally. We first compared the cellular localization of the intact EBNA-1 (aa 1 to 641) with that of three variants that were deleted for sequences between aa 390 and 547, 329 and 345, and 430 and 641. cos cells were transfected with the plasmid constructions and stained for EBNA-1 in an indirect immunofluorescence assay. Each of these EBNA-1 polypeptides retained the property of nuclear localization (Table 1). This result indicated that a nuclear localization signal must lie either in the aa 1 to 328 or 345 to 390 region of the protein. However, it did not eliminate the possibility of a second signal occurring in the carboxy-terminal region. To address this possibility, a pyruvate kinase vector system was employed. Pyruvate kinase is a cytoplasmic protein (Fig. 7A, Table 1) that can be relocated to the nucleus by the addition of a nuclear localization signal, for example, that from the c-*myc* proto-oncogene (Fig. 7B). When the aa 450 to 641 region of EBNA-1 was linked in phase to pyruvate kinase, a fusion protein was formed that localized to the cytoplasm of transfected cells (Fig. 7D). Therefore, the 450-641 polypeptide carboxy terminus does not contain a nuclear localization signal. This EBNA-1 polypeptide could, however, be artificially moved to the nucleus by placing the same EBNA-1 carboxy-terminal coding sequences into a pyruvate kinase vector containing the c-*myc* nuclear localization signal (Fig. 7E).

Identification of the nuclear localization signal. Transfection experiments with the deleted variants of EBNA-1 (Table 1) had indicated that a nuclear localization signal must exist in regions comprising aa 1 to 328 or 345 to 390. The central one-third of EBNA-1 (aa 90 to 328) is composed of a repetitive Gly-Gly-Ala domain, and this effectively limited the areas of interest to aa 1 to 89 and 345 to 390. Nuclear localization signals characteristically contain positively charged amino acids, and the most promising blocks of sequence within the aa 1 to 89 and 345 to 390 regions occurred at aa 71 to 77 and 379 to 387, respectively. The abilities of these sequences to confer nuclear localization were tested by introducing them into a vector that expresses a deleted, predominantly cytoplasmic localizing variant of the HSV immediate-early protein, IE175. Wild-type IE175 is a nuclear protein (Fig. 8A and Table 2), while the ΔIE175 vector (pGH115) expresses a protein that localizes predominantly to the cytoplasm in transfected cells (Fig. 8B) but also exhibits mixed cytoplasmic-nuclear staining in a small

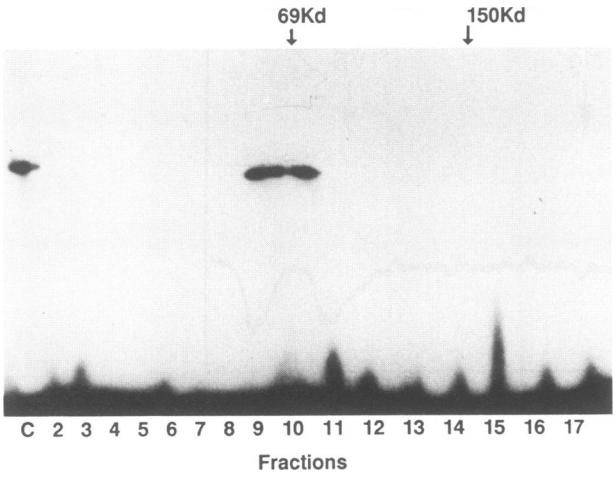

FIG. 5. Examination of 28K EBNA-1 by velocity sedimentation. Mobility retardation assay performed on 10-μl aliquots of each fraction from a 10 to 30% glycerol gradient containing the bacterially expressed EBNA-1 (aa 450 to 641). The relative sedimentation positions of bovine serum albumin (69 kDa) and alcohol dehydrogenase (150 kDa) marker proteins are shown. The location of the binding activity in the gradient indicates that EBNA-1 (aa 450 to 641) behaves as a 53- to 70-kDa protein and confirms the multimeric nature of EBNA-1 in solution.

proportion of cells. None of the ΔIE175-transfected cells showed exclusively nuclear staining, and hence we chose to utilize this criterion as a measure of transfer of a functional localization signal. Vero cells transfected with these plasmids were stained for HSV IE175 in an indirect immunofluorescence assay. The ΔIE175 protein containing an in-phase insertion of EBNA-1 aa 71 to 77 localized to the cytoplasm, as did the parental vector (Fig. 8C). However, the IE175 variant fused to aa 379 to 387 of EBNA-1 showed exclusive nuclear staining (Fig. 8E). An additional relatively positively charged amino acid sequence occurs at aa 394 to 405. To address the possibility of multiple nuclear localization signals, this sequence was also tested in the HSV IE175 vector, but it did not confer nuclear localization (Fig. 8F). To address the issue of specificity, the oligonucleotide inserts encoding EBNA-1 aa 71 to 77, 379 to 387, and 394 to 405 were also introduced into the IE175 vector in the reverse orientation. No nuclear localization was observed with the reverse constructions (Fig. 8D). However, it should be noted that the reverse orientation of the aa 379 to 387 insert introduced a terminator, and in fact no staining, cytoplasmic or nuclear, was observed in cells transfected with this construction. This negative result is consistent with the fact that the epitope for the monoclonal antibody being used in the immunofluorescence assay lies downstream of the terminator and would not be expressed from the reversed insert construction. As an additional test of specificity, a positively charged sequence (aa 457 to 462) from within the aa 450 to 641 domain of EBNA-1 that had tested negative for nuclear localization was introduced into the pyruvate kinase vector. Consistent with the earlier observation, the expressed pyruvate kinase protein containing this signal remained cytoplas-

TABLE 1. Carboxy terminus of EBNA-1 (aa 450 to 641) does not contain a nuclear localization signal

Plasmid	Description[a]	EBNA-1 insert (aa)	Nuclear
pRA17	CMV–EBNA-1	1–641	Yes
pRA31	CMV–EBNA-1	1–429	Yes
pRA35	CMV–EBNA-1	1–389, 548–641	Yes
pRA37	CMV–EBNA-1	1–328, 346–641	Yes
pRLPK12	SV-PK	None	No
pRA315	SV-*myc* NLS-PK	None	Yes
pRA321	pRLPK12–EBNA-1	450–641	No
pRA336	pRA315–EBNA-1	450–641	Yes

[a] CMV, Cytomegalovirus; SV, simian virus 40; *myc* NLS, nuclear localization signal from *myc* oncogene; PK, pyruvate kinase.

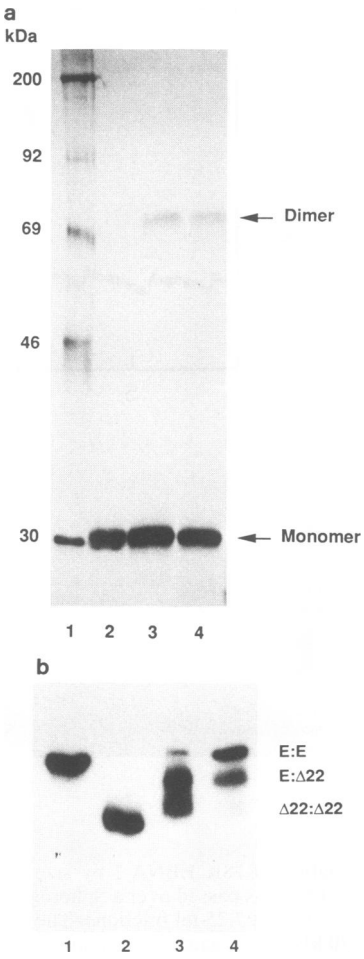

FIG. 6. EBNA-1 forms dimers and binds to DNA as a dimer. EBNA-1 was prepared by in vitro transcription and translation, and the nature of the oligomeric complex was further probed in cross-linking and heterodimerization assays. (a) ^{35}S-labeled EBNA-1 (aa 408 to 641) was immunoprecipitated with rabbit anti-EBNA-1 antiserum from the in vitro translation mixture either before (lane 2) or after (lanes 3 and 4) cross-linking with glutaraldehyde and subjected to electrophoresis on a denaturing 12% acrylamide gel. Relative to the marker proteins (lane 1), the cross-linked form of EBNA-1 migrated as a dimer. (b) Mobility retardation assay performed with the standard 30-mer-oligonucleotide probe and EBNA-1 (aa 408 to 641) (lane 1), Δ22 EBNA-1 (aa 408 to 619) (lane 2), cotranslated EBNA-1 (aa 408 to 641) plus Δ22 EBNA-1 in a 1:2 ratio (lane 3), and cotranslated EBNA-1 (aa 408 to 641) plus Δ22 EBNA-1 in a 2:1 ratio (lane 4). In this experiment, the probe oligonucleotide has been run off the gel. The formation of a complex with an intermediate mobility (E:Δ22) indicates that EBNA-1 is binding DNA as a dimer.

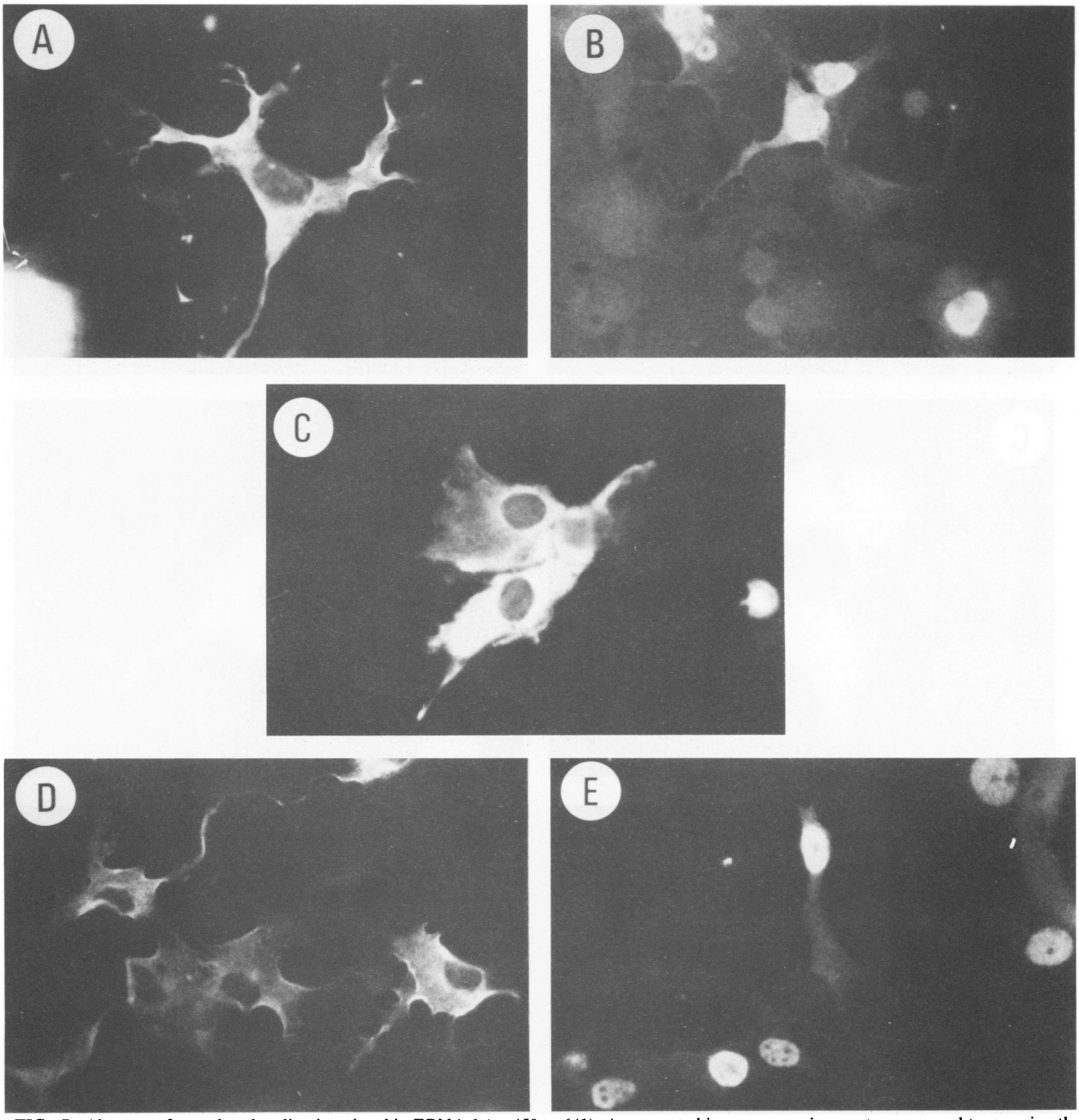

FIG. 7. Absence of a nuclear localization signal in EBNA-1 (aa 450 to 641). A pyruvate kinase expression vector was used to examine the intracellular localization of constructions containing all, or a portion, of the aa 450 to 641 segment of EBNA-1. cos-7 cells were transfected with the pyruvate kinase expression vector pRLPK12 (A) or the pyruvate kinase vector containing the *myc* nuclear localization signal (pRA315) (B), containing an insert expressing aa 457 to 462 of EBNA-1 (pRA298) (C), expressing EBNA-1 (aa 450 to 641) (pRA321) (D), or expressing both the *myc* nuclear localization signal and EBNA-1 (aa 450 to 641) (pRA336) (E). Cells were stained 48 h after transfection by using rabbit anti-pyruvate kinase antiserum in an indirect immunofluorescence assay. The data are summarized in Tables 1 and 2.

mic (Fig. 7C and Table 2). These results establish that a nuclear localization signal for EBNA-1 is located between aa 379 and 387 (Table 2). Data from the signal transfer experiments were consistent with those from the deletional experiments, which suggests that EBNA-1 probably does not contain more than one nuclear localization signal.

Carboxy-terminal 191 aa contain a transactivator domain. EBNA-1 is capable of transactivating expression from a target plasmid containing EBNA-1-binding sites, and a commonly used target reporter gene is the FRTK-CAT of Reisman and Sugden (33) that contains the family of repeats from ori-P located downstream from the *cat* gene in a

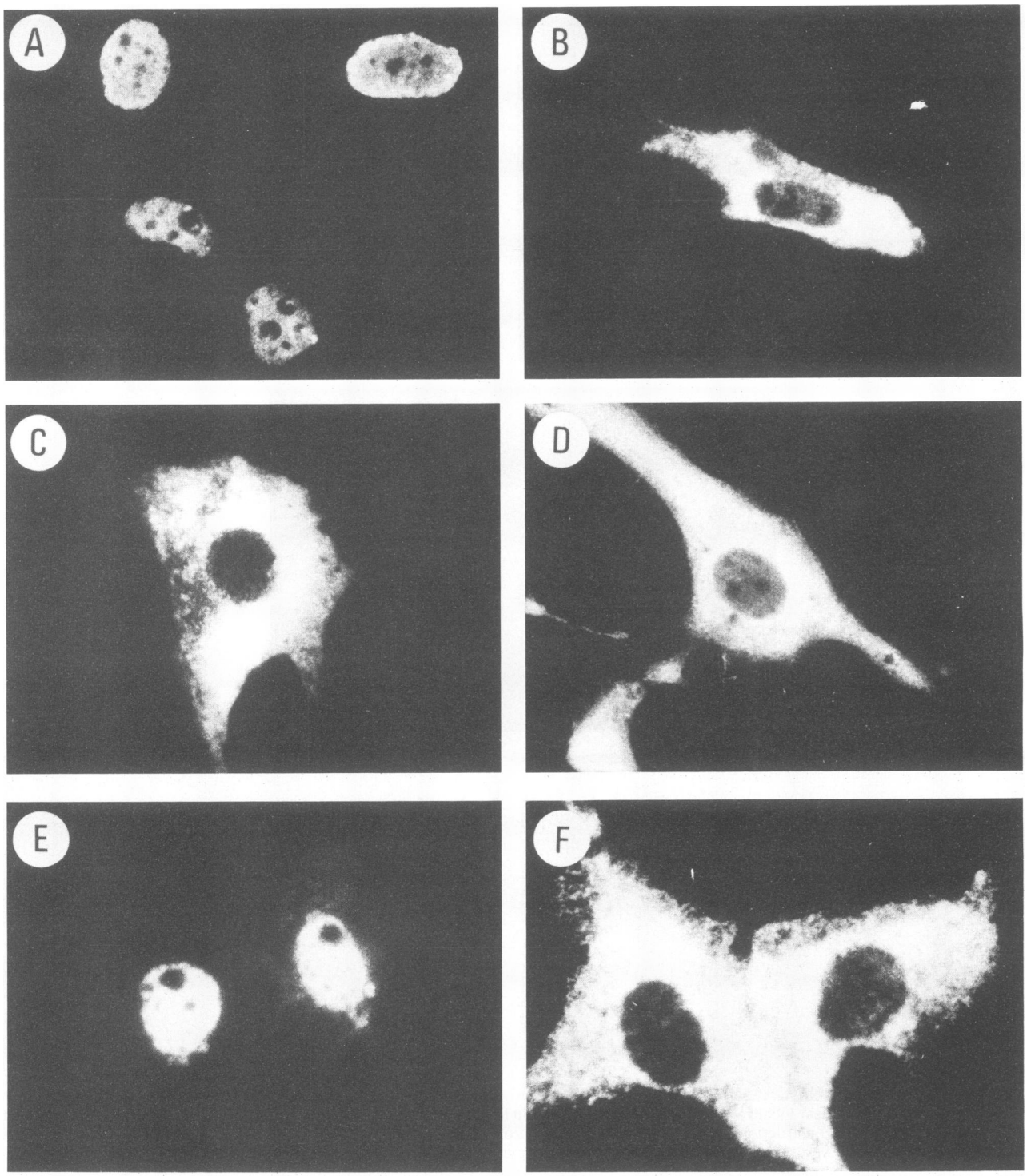

FIG. 8. aa 379 to 386 of EBNA-1 are sufficient to confer nuclear localization. An HSV ΔIE175 expression vector was used to examine the ability of positively charged amino acid blocks within EBNA-1 to confer the characteristic of nuclear localization. Vero cells were transfected with the IE175 constructions and stained 48 h later with monoclonal antibody against IE175 (36) in an indirect immunofluorescence assay. (A) Wild-type IE175; (B) ΔIE175; (C) ΔIE175–EBNA-1 (aa 71 to 77); (D) ΔIE175–EBNA-1 (aa 71 to 77 in the antisense orientation); (E) ΔIE175–EBNA-1 (aa 379 to 386); (F) ΔIE175–EBNA-1 (aa 394 to 405). The data are summarized in Table 2.

TK-CAT construction. Transactivation is dependent on the presence of the DNA-binding domain of EBNA-1, since deletion of aa 430 to 641 abolishes activity (Fig. 9a). The ability of the EBNA-1 450-641 fusion polypeptide to activate FRTK-CAT was examined in a short-term cotransfection assay in Vero cells. Transactivation was observed when the aa 450 to 641 region was expressed as a pyruvate kinase fusion protein containing a nuclear localization signal, but

TABLE 2. Identification of EBNA-1 nuclear localization signal

Plasmid	Description[a]	EBNA-1 insert	% Nuclear[b]
pGH114	HSV IE175	None	100
pGH115	HSV ΔIE175	None	0
pMAH9a	ΔIE175 + -RRPQKRP-	bp 211–231; aa 71–77	0.5
pMAH9b	ΔIE175 + -GRFWGLR-	bp 231–211	0
pMAH10a	ΔIE175 + -KRPRSPSS-	bp 1135–1158; aa 379–386	55
pMAH10b	ΔIE175 + -*-	bp 1158–1135	—[c]
pMM15a	ΔIE175 + -SPPRRPPPGRRP-	bp 1177–1212; aa 394–405	0
pMM15b	ΔIE175 + -CGLLPGGGLRGG-	bp 1212–1177	0
pRA298	SV-PK + -GRRKKG-	bp 1369–1386; aa 457–462	0

[a] IE175 peptides were detected with monoclonal antibody 58S; pyruvate kinase (PK) peptides were detected with rabbit anti-pyruvate kinase antibody. *, translational terminator; SV, simian virus 40.
[b] Fluorescent cells with exclusively nuclear staining.
[c] —, Truncated peptide not recognized by 58S antibody.

only low levels of activation were seen when the equivalent construction lacking the localization signal was used (Fig. 9b). We conclude that efficient nuclear localization improves EBNA-1 transactivation function and that an activation domain exists within the aa 450 to 641 carboxy-terminal region of the protein. EBNA-1 contains a negatively charged tail, aa 600 to 641, in which 17 of the 41 amino acids are either glutamate or aspartate. This region can be deleted without destroying the transactivation function of the otherwise intact protein [Fig. 10, EBNA (1-604)]. To test whether this domain was contributing to transactivation by the 450-641 polypeptide, a variant, EBNA (450-604), which lacked the bulk of the acidic domain, was created. The FRTK-CAT target had a reduced response to cotransfection with the truncated polypeptide (Fig. 10), suggesting that the negative tail contributed an activator function. A summary of the domain mapping data described in this report is presented in Fig. 11.

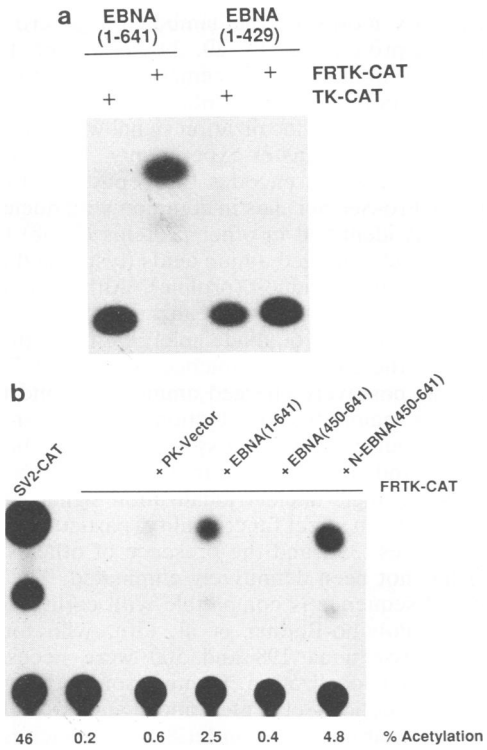

FIG. 9. EBNA-1 (aa 450 to 641) forms a functional transactivator. Cotransfection assays were performed in Vero cells using either a nonspecific target (TK-CAT) or TK-CAT plus the EBNA-1-binding sites from the family of repeats (FRTK-CAT). CAT activity was determined 48 h after transfection. (a) FRTK-CAT but not TK-CAT is transactivated by intact EBNA-1 (aa 1 to 641). Truncation of EBNA-1 at aa 429 [EBNA-1 (1-429)] abolishes transactivation. Cells were transfected with 2 μg of target and 2 μg of activator plasmid. (b) The carboxy terminus of EBNA-1 is sufficient to produce a transactivation response if a nuclear location signal is provided [N-EBNA (450-641)] but is not active in the absence of this signal [EBNA (450-641)]. Cells were transfected with control SV2-CAT (2 μg) or with 0.25 μg of FRTK-CAT and 2 μg of activator plasmid.

DISCUSSION

EBNA-1 plays an intimate role in the maintenance of latent EBV infection. The dyad symmetry region of ori-P, which is the site of initiation of episomal EBV DNA replication, contains 4 binding sites for EBNA-1, and the enhancer domain of the origin, which contributes to transcriptional activation of the *Bam*HI-C latency promoter, contains

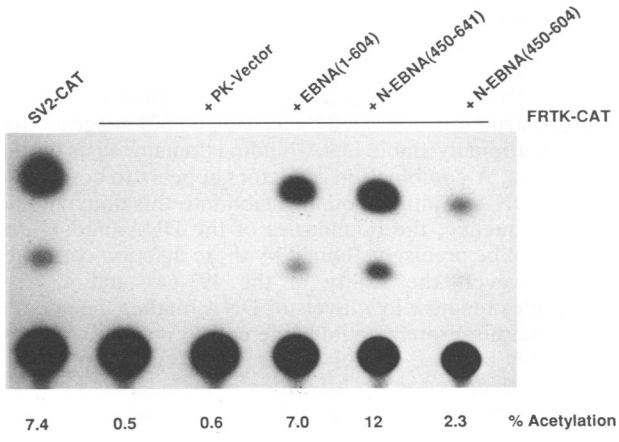

FIG. 10. A negatively charged terminal domain, aa 605 to 641, contributes to transactivation by EBNA-1 (aa 450 to 641). Cotransfection assays were performed as described in the legend to Fig. 9b, except that 0.5 μg of control SV2-CAT was used. Transactivation by the nuclear N-EBNA (aa 450 to 641) was significantly diminished by removal of the terminal 37 aa [N-EBNA (450-604)]. However, removal of this domain from the intact protein [EBNA (1-604)] did not ablate transactivation function.

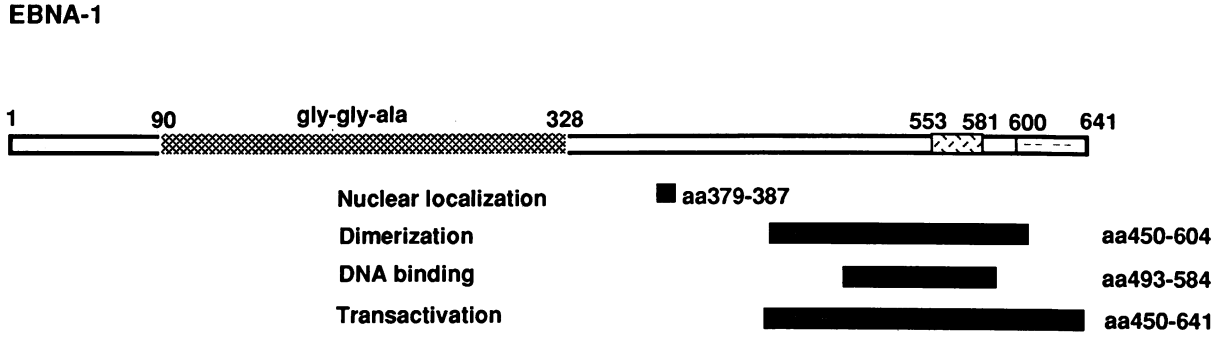

FIG. 11. Summary of the EBNA-1 domain mapping experiments. Diagrammatic representation of the 641-aa EBNA-1 polypeptide. Symbols: ▩, repeat domain composed entirely of glycine and alanine residues; ▨, potential leucine zipper dimerization motif; --, negatively charged region in which 17 of 41 amino acids are either aspartate or glutamate. The minimal active domains that were defined in these studies are shown as solid bars.

20 EBNA-1-binding sites. Given that binding of EBNA-1 to its target recognition sequence is crucial for EBNA-1 function, characterization of this interaction is of some interest. In these studies we used chromatographic, sedimentation, cross-linking, and heterodimerization techniques to demonstrate that an EBNA-1 variant comprising the carboxy-terminal 191 aa of EBNA-1 exists in solution as a dimer and also binds to its specific recognition sequence as a dimer. That the active binding form of EBNA-1 is a dimer is compatible with previous data showing that increasing or decreasing the spacing between the halves of the palindromic DNA recognition sequence destroyed binding (3) and is also compatible with the pattern of methylation interference exhibited by bound EBNA-1 (3, 18). The necessity for EBNA-1 to dimerize to have biological activity raises the possibility of using EBNA-1 variants which dimerize but lack DNA-binding or transactivation function as transdominant inhibitors to block EBNA-1 activity and hence potentially cure latently infected cells. Transdominant inhibition has been demonstrated to be effective in a model system when the HSV virion factor Vmw65 was used. Introduction of a virion factor mutant that was deleted for the transactivation domain blocked progression of a subsequent HSV-1 infection in tissue culture (10).

Deletional analyses provided information on the location of the DNA-binding domain. The retention of wild-type levels of DNA binding and maintenance of protein stability in the constructions bounded by aa 459 and 607 suggests that a conformationally stable DNA-binding domain exists within these 148 aa. A combination of factors appears to contribute to loss of DNA binding upon intrusion into this domain, and as a consequence, the boundaries of the DNA-binding domain cannot be precisely defined by these deletion constructions. However, the ability of the 493-641 and 450-584 polypeptides to show low levels of DNA binding despite the fact that neither protein could be detected on an immunoblot (presumably because of their lack of stability) is interpreted to indicate that a core DNA-binding domain exists between aa 493 and 584 of EBNA-1. Since DNA binding requires EBNA-1 dimerization, this 91-aa domain presumably comprises two subdomains: one that makes contact with the DNA duplex and a second that is involved in protein-protein dimerization. One recognized mechanism for protein dimerization is via a leucine zipper, which comprises leucine residues spaced 7 aa apart (19). Functional zippers in which some of the leucines are replaced by other hydrophobic residues have also been described (4). A potential modified leucine zipper motif, Leu-Tyr-Thr-Leu-Leu, with the appropriate heptad spacing, exists between aa 553 and 581. Preliminary evidence supports a correlation between this subdomain and dimerization ability (36a). The region comprising aa 493 to 527 has a predicted overall alpha-helical structure, and it shows a limited degree of homology to the helix-turn-helix motifs of the lambda phage cro and rep DNA-binding proteins (1, 16, 20, 29). However, the exact nature of the binding motif remains speculative in the absence of supporting experimental data.

The EBNA-1 nuclear localization signal was mapped to aa 379 to 386 by using transfer experiments. This karyophilic signal sequence, which encodes the peptide Leu-Lys-Arg-Pro-Arg-Ser-Pro-Ser-Ser, has in common with nuclear localization signals identified in other proteins (7, 38) the presence of positively charged amino acids (lysine and arginine) and helix-breaking residues (proline). Although these are recognized features of nuclear localization signals, a prediction of function cannot be made solely on these properties. For example, the EBNA-1 sequence between aa 71 and 77 contains four positively charged amino acids and two prolines, yet this region did not function as a nuclear localization signal in our experimental system. The combined peptide transfer and deletion data implied that EBNA-1 may contain only a single nuclear localization signal. However, protein context can affect functionality, particularly of weak signal sequences (35), and the presence of other signals in EBNA-1 has not been definitively eliminated. The location of the signal sequence is compatible with earlier deletional analyses by Polvino-Bodnar et al. (30), who found that sequences between aa 198 and 500 were necessary for correct EBNA-1 localization. Comparison with two of the deletion constructions of Yates and Camiolo (44) is also informative. Their construction DL8DL89, which is deleted for aa 384 to 391 and 432 to 451, functioned at approximately 80% of the efficiency of the wild-type protein in transient replication, enhancer, and plasmid maintenance assays. Assuming that nuclear localization of EBNA-1 is a requirement for each of these functions, this result implies either that the 3′ 3 aa of our 8-aa nuclear localization signal (Pro-Ser-Ser) may not be essential or that they can be replaced by Gly-Ser-Pro, as occurs in the DL8DL89 construction. The second relevant plasmid, DL45, is deleted for aa 329 to 381, which removes the 5′ 3 aa (Lys-Arg-Pro) from the nuclear localization signal identified here. The impaired functionality of the DL45 construction (it scored negative for plasmid maintenance and 10-fold lower than wild type in the en-

hancer activation assay) would be compatible with a nuclear localization signal mapping at aa 379 to 386.

The transactivation experiments were directed toward one particular issue: whether the carboxy-terminal one-third of EBNA-1 was capable of functioning as a transactivator. The design of these experiments was complicated by the fact that we were unable to obtain stable expression of an aa 450 to 641 EBNA-1 variant in eukaryotic cells (unpublished observations). The aa 450 to 641 region could, however, be stabilized by formation of a fusion protein, and the vector used in the transfection experiments was one expressing pyruvate kinase. When provided with a nuclear localization signal, this aa 450 to 641 segment of EBNA-1 gave a 24-fold activation of a FRTK-CAT target in cotransfection assays. Interestingly, the activation was significantly reduced by removal of aa 605 to 641. This 41-aa tail contains 17 negatively charged aa, and negatively charged domains have been implicated in the transactivator function of a variety of cellular and viral transactivator proteins (12, 31). However, as reported by others (30, 44) and as shown here, removal of the terminal 41 aa from an otherwise intact EBNA-1 protein does not ablate transactivation. Thus, EBNA-1 apparently contains two physically distinct activator domains, one located between aa 605 and 641 and a second located outside of the aa 450 to 641 region that was examined in this series of experiments.

Beyond its ability to bind specifically to DNA, little is understood of the mechanistic contribution of EBNA-1 to DNA replication or transactivation. EBNA-1 has not been demonstrated to exhibit any of the enzymatic properties associated with other viral replication proteins such as simian virus 40 T antigen (32a). Accumulation of fundamental information, such as on the domain structure of EBNA-1, provides a basis for future probing into the functioning of this key latency protein.

ACKNOWLEDGMENTS

We acknowledge Mabel Chiu, Jian Zhang, and Beverley Lambe for excellent technical assistance; Waris Shah for generously providing purified 28K EBNA-1; and Linda Kelly and Pamela Wright for manuscript preparation.

These studies were funded by Public Health Service grants K11 AI00648 (R.A.), RO1CA28473 (G.S.H.), and RO1CA42245 (S.D.H.) from the National Institutes of Health. R.A. received support from Caswell Caplan and the Hodson Trust.

REFERENCES

1. **Aggarwal, A. K., D. W. Rodgers, M. Drottar, M. Ptashne, and C. Harrison.** 1988. Recognition of a DNA operator by the repressor of phage 434: a view at high resolution. Science **242**:899–907.
2. **Ambinder, R. F., W. A. Shah, E. D. Fixman, B. C. Lambe, D. R. Rawlins, G. S. Hayward, and S. D. Hayward.** 1989. DNA: EBNA-1 interactions and latency of Epstein Barr virus, p. 37–42. *In* D. Ablashi et al. (ed.), Epstein-Barr virus and human disease, vol. II. Humana Press, N.J.
3. **Ambinder, R. F., W. A. Shah, D. R. Rawlins, G. S. Hayward, and S. D. Hayward.** 1990. Definition of the sequence requirements for binding of the EBNA-1 protein to its palindromic target sites in Epstein-Barr virus DNA. J. Virol. **64**:2369–2379.
4. **Chang, Y.-N., D. L.-Y. Dong, G. S. Hayward, and S. D. Hayward.** 1990. The EBV Zta transactivator: a member of the bZIP family with unique DNA binding specificity and a dimerization domain that lacks the characteristic heptad leucine zipper motif. J. Virol. **64**:3358–3369.
5. **Chen, C., and H. Okayama.** 1987. High-efficiency transformation of mammalian cells by plasmid DNA. Mol. Cell. Biol. **7**:2745–2752.
6. **Chittenden, T., S. Lupton, and A. J. Levine.** 1989. Functional limits of *oriP*, the Epstein-Barr virus plasmid origin of replication. J. Virol. **63**:3016–3025.
7. **Dang, C. V., and W. M. F. Lee.** 1989. Nuclear and nucleolar targeting sequences of c-erb-A, c-myb, N-myc, p53, HSP70, and HIV tat proteins. J. Biol. Chem. **264**:18019–18023.
8. **Dasmahapatra, D. B., E. J. Rozhan, and J. Schwarz.** 1987. pBD7, a novel cell free expression vector with an efficient translation initiation signal. Nucleic Acids Res. **15**:3933.
9. **Farrel, P. J.** 1989. Epstein-Barr Virus genome, p. 103–132. *In* G. Klein (ed.), Advances in viral oncology, vol. 8. Raven Press, Ltd., N.Y.
10. **Friedman, A. D., S. J. Triezenberg, and S. L. McKnight.** 1988. Expression of a truncated viral transactivator selectively impedes lytic infection by its cognate virus. Nature (London) **335**:452–454.
11. **Gahn, T. A., and C. L. Schildkraut.** 1989. The Epstein-Barr virus origin of plasmid replication, ori-P, contains both the initiation and termination sites of DNA replication. Cell **58**:527–535.
12. **Gill, G., and M. Ptashne.** 1987. Mutants of GAL4 protein altered in an activation function. Cell **51**:121–126.
13. **Hope, I. A., and K. Struhl.** 1987. GCN4, a eukaryotic transcriptional activator protein, binds as a dimer to target DNA. EMBO **6**:2781–2784.
14. **Jeang, K.-T., D. R. Rawlins, P. J. Rosenfeld, J. H. Shero, T. J. Kelly, and G. S. Hayward.** 1987. Multiple tandemly repeated binding sites for cellular nuclear factor 1 that surround the major immediate-early promoters of simian and human cytomegalovirus. J. Virol. **61**:1559–1570.
15. **Jones, C. H., S. D. Hayward, and D. R. Rawlins.** 1989. Interaction of lymphocyte-derived Epstein-Barr virus nuclear antigen (EBNA-1) with its DNA-binding sites. J. Virol. **63**:101–110.
16. **Jordan, S. R., and C. O. Pabo.** 1988. Structure of the lambda complex at 2.5Å resolution. Details of the repressor-operator interactions. Science **242**:893–899.
17. **Kieff, E., and D. Liebowitz.** 1990. Epstein-Barr virus and its replication, p. 1889–1920. *In* B. N. Fields, D. M. Knipe, et al. (ed.), Virology, 2nd ed. Raven Press, N.Y.
18. **Kimball, A. S., G. Milman, and T. D. Tullius.** 1989. High-resolution footprints of the DNA-binding domain of Epstein-Barr virus nuclear antigen 1. Mol. Cell. Biol. **9**:2738–2742.
19. **Landschulz, W. H., P. F. Johnson, and S. L. McKnight.** 1988. The leucine zipper: a hypothetical structure common to a new class of DNA-binding proteins. Science **240**:1759–1764.
20. **Lawrence, J. B., C. A. Villnave, and R. H. Singer.** 1988. Sensitive, high resolution chromatin and chromosome mapping *in situ*: presence and orientation of two closely integrated copies of EBV in a lymphoma line. Cell **52**:51–61.
21. **Lindahl, T., A. Adams, G. Bjursell, G. W. Bornkamm, C. Kaschaka-Dierich, and U. Jehn.** 1976. Covalently closed circular duplex DNA of Epstein-Barr virus in a human lymphoid cell line. J. Mol. Biol. **102**:511–530.
22. **Lupton, S., and A. J. Levine.** 1985. Mapping genetic elements of Epstein-Barr virus that facilitate extrachromosomal persistence of Epstein-Barr virus-derived plasmids in human cells. Mol. Cell. Biol. **5**:2533–2542.
23. **Maniatis, T., E. F. Fritsch, and J. Sambrook.** 1982. Molecular cloning: a laboratory manual, p. 202. Cold Spring Harbor Laboratory, Cold Spring Harbor, N.Y.
24. **Matsuo, T., M. Heller, L. Petti, E. Oshiro, and E. Kieff.** 1984. Persistence of the entire EBV genome integrated into human lymphocyte DNA. Science **226**:1322–1325.
25. **Milman, G., and E. S. Hwang.** 1987. Epstein-Barr virus nuclear antigen forms a complex that binds with high concentration dependence to a single DNA-binding site. J. Virol. **61**:465–471.
26. **Milman, G., A. L. Scott, M. S. Cho, S. C. Hartman, D. K. Ades, G. S. Hayward, P. G. Ki, J. T. August, and S. D. Hayward.** 1985. Carboxyl-terminal domain of the Epstein-Barr virus nuclear antigen is highly immunogenic in man. Proc. Natl. Acad. Sci. USA **82**:6300–6304.
27. **Nonoyama, M., and J. S. Pagano.** 1972. Separation of Epstein-Barr virus DNA from large chromosomal DNA in non-virus-

producing cells. Nature (London) New Biol. **238**:169–171.
28. **O'Hare, P., and G. S. Hayward.** 1985. Evidence for a direct role for both the 175,000- and 110,000-molecular-weight immediate-early proteins of herpes simplex virus in the transactivation of delayed early promoters. J. Virol. **53**:751–760.
29. **Pabo, C. O., and R. T. Saur.** 1984. Protein-DNA recognition. Annu. Rev. Biochem. **53**:293–321.
30. **Polvino-Bodnar, M., J. Kiso, and P. A. Schaffer.** 1988. Mutational analysis of Epstein-Barr virus nuclear antigen 1 (EBNA-1). Nucleic Acids Res. **16**:3415–3435.
31. **Ptashne, M.** 1988. How eukaryotic transcriptional activators work. Nature (London) **335**:683–689.
32. **Rawlins, D. R., G. Milman, S. D. Hayward, and G. S. Hayward.** 1985. Sequence-specific DNA binding of the Epstein-Barr virus nuclear antigen (EBNA-1) to clustered sites in the plasmid maintenance region. Cell **42**:859–868.
32a. **Rawlins, D. R., and W. Shah.** Unpublished data.
33. **Reisman, D., and B. Sugden.** 1986. *trans*-activation of an Epstein-Barr viral (EBV) transcriptional enhancer by the EBV nuclear antigen 1. Mol. Cell. Biol. **6**:3838–3846.
34. **Reisman, D., J. Yates, and B. Sugden.** 1985. A putative origin of replication of plasmids derived from Epstein-Barr virus is composed of two *cis*-acting components. Mol. Cell. Biol. **5**:410–413.
35. **Roberts, B. L., W. D. Richardson, and A. E. Smith.** 1987. The effect of protein context on nuclear location signal function. Cell **50**:465–475.
36. **Sample, J., M. Hummel, D. Braun, M. Birkenbach, and E. Kieff.** 1986. Nucleotide sequences of messenger RNAs encoding Epstein-Barr virus nuclear proteins: a probable transcriptional initiation site. Proc. Natl. Acad. Sci. USA **83**:5096–5100.
36a. **Shah, W.** Unpublished data.
37. **Showalter, S. D., M. Zweig, and B. Hampar.** 1981. Monoclonal antibodies to herpes simplex virus type 1 proteins including the immediate-early protein ICP4. Infect. Immun. **34**:684–692.
38. **Smith, A. E., D. Kalderon, B. L. Roberts, W. H. Colledge, M. Edge, P. Gillett, A. Markham, E. Paucha, and W. D. Richardson.** 1985. The nuclear location signal. Proc. R. Soc. London B **226**:43–58.
39. **Speck, S., and J. Strominger.** 1985. Analysis of the transcript encoding the latent Epstein-Barr virus nuclear antigen I: a potentially polycistronic message generated by long range splicing of several exons. Proc. Natl. Acad. Sci. USA **82**:8305–8309.
40. **Sugden, B., and N. Warren.** 1989. A promoter of Epstein-Barr virus that can function during latent infection can be transactivated by EBNA-1, a viral protein required for viral DNA replication during latent infection. J. Virol. **63**:2644–2649.
41. **Summers, W. P., E. A. Grogan, D. Shedd, M. Robert, C. R. Liu, and G. Miller.** 1982. Stable expression in mouse cells of nuclear neoantigen after transfer of a 3.4-megadalton cloned fragment of Epstein-Barr virus DNA. Proc. Natl. Acad. Sci. USA **79**:5688–5692.
42. **Wysokenski, D. A., and J. L. Yates.** 1989. Multiple EBNA1-binding sites are required to form an EBNA1-dependent enhancer and to activate a minimal replicative origin within *oriP* of Epstein-Barr virus. J. Virol. **63**:2657–2666.
43. **Yates, J., N. Warren, D. Reisman, and B. Sugden.** 1984. A cis-acting element from the Epstein-Barr viral genome that permits stable replication of recombinant plasmids in latently infected cells. Proc. Natl. Acad. Sci. USA **81**:3806–3810.
44. **Yates, J. L., and S. M. Camiolo.** 1988. Dissection of DNA replication and enhancer activation functions of Epstein-Barr virus nuclear antigen 1. Cancer Cells **6**:197–205.
45. **Yates, J. L., N. Warren, and B. Sugden.** 1985. Stable replication of plasmids derived from Epstein-Barr virus in a variety of mammalian cells. Nature (London) **313**:812–815.